

UNCLASSIFIED

RM No. L7C24a

APR 25 1947



CR
~~6440~~
~~1472~~

RESEARCH MEMORANDUM

INVESTIGATION OF INTAKE DUCTS FOR A HIGH-SPEED

SUBSONIC JET-PROPELLED AIRPLANE

By Herbert N. Cohen

Langley Memorial Aeronautical Laboratory
Langley Field, Va.

CLASSIFICATION CANCELLED

CLASSIFIED DOCUMENT

This document contains classified information affecting the National Defense of the United States within the meaning of the Espionage Act, USC 50:31 and 32. Its transmission or the revelation of its contents in any manner to an unauthorized person is prohibited by law. Information so classified may be imparted only to persons in the military or naval services of the United States, appropriate civilian officers and employees of the Federal Government who have a legitimate interest therein, and to United States citizens of known loyalty and discretion who of necessity must be informed thereof.

Authority J. W. Crowley Date 12/14/53
J. E. G. 1052
note 1/18/54 See NACA
R 7 2106

NATIONAL ADVISORY COMMITTEE FOR AERONAUTICS

WASHINGTON

April 23, 1947

NACA LIBRARY
LANGLEY MEMORIAL AERONAUTICAL
LABORATORY
Langley Field, Va.

UNCLASSIFIED

NATIONAL ADVISORY COMMITTEE FOR AERONAUTICS

RESEARCH MEMORANDUM

INVESTIGATION OF INTAKE DUCTS FOR A HIGH-SPEED
SUBSONIC JET-PROPELLED AIRPLANE

By Herbert N. Cohen

SUMMARY

Results of pressure-loss measurements are presented for full-scale models of two alternate ducts under consideration for use in the induction system of an experimental jet-propelled airplane designed for flight at high subsonic speeds. Supplementary pressure-loss measurements were made on the better of the two ducts, designated duct II, first with carborundum grains in the duct inlet and then with a spoiler in order to obtain an indication of the importance of inlet roughness and surface discontinuities. Additional measurements were made of duct II incorporating a horizontal "splitter" vane which was under consideration for structural reasons.

For standard sea-level inlet conditions, the pressure loss for duct II at the maximum test air-flow rate of 27 pounds per second was about 8 pounds per square foot or only 37 percent of the loss for duct I. The pressure losses of duct II were increased approximately 50 percent by the installation of the splitter vane or the use of the carborundum grains and about 700 percent by the use of the spoiler.

INTRODUCTION

In the design of an experimental jet-propelled airplane intended for flight at high subsonic speeds, several alternate duct geometries for use in the air-induction system have been under consideration. Pressure losses of full-scale models of the proposed ducts were therefore measured in order that their suitability to the requirements of the airplane might be evaluated. The airplane, which has a jet engine located in the fuselage directly behind the pilot's seat, is illustrated as figure 1. The air-induction system has a single nose inlet, immediately behind which the duct divides to pass around the pilot's seat and wheel well and joins again at the inlet to the jet engine. Wind-tunnel tests of a similar arrangement were previously reported in reference 1. The duct designated duct I was designed to minimize the frontal area of the airplane and necessarily operated at high internal flow velocities.

Estimates of the performance of this duct based on data such as those of reference 2 indicated that the internal losses would be excessive. Duct II was therefore designed to incorporate larger internal passages, wherever possible, in order to reduce the ducting losses. This increase in duct area was accomplished at the expense of a 20-percent increase in fuselage frontal area; it was believed, however, that this increase could be effected without impairing the performance of the airplane.

The pressure losses for both ducts were measured over a range of weight rate of air flow. In order to obtain an indication of the effects of finish and workmanship on the ducts, pressure losses of the second duct were also measured first with carborundum grains and then with a spoiler in the duct inlet. Measurements of the second duct were then repeated after installing a long horizontal "splitter" vane which was under consideration for structural reasons.

The investigation was conducted at the Langley induction aerodynamics laboratory of the NACA.

SYMBOLS

H	total pressure, pounds per square foot
\bar{H}	average total pressure, pounds per square foot
q	dynamic pressure, pounds per square foot $\left(\frac{1}{2}\rho V^2\right)$
V	velocity, feet per second
W	weight rate of air flow, pounds per second
ρ	mass density of air, slugs per cubic foot
σ_1	relative density, that is, ratio of density of air at duct inlet to standard density (ρ_1/ρ_0)

Subscripts:

e	at duct exit
i	at duct inlet
l	any local point in a duct section

O for standard sea-level conditions (29.92 in. Hg absolute pressure and 60° F temperature)

max maximum

MODELS AND APPARATUS

Lines of the original duct (duct I) and the redesigned duct (duct II) are shown in figures 2(a) and 2(b), respectively. Only the right half of the symmetrical ducts was reproduced for the tests. Views of the inlets for both ducts and of the exit for duct I are shown in figures 3 and 4, respectively. The short rear splitter vane for duct I, indicated in figure 2(a), is shown also in figure 4. The long horizontal splitter vane that was considered for use with duct II is indicated by the short dashed lines in figure 2(b) and is shown in a disassembled view of the duct in figure 5. Cross-sectional areas and hydraulic diameters for several stations of duct I, duct II, and duct II with the splitter vane are given in table I.

The test setup is shown in a diagrammatic sketch in figure 6(a) and in a photograph in figure 6(b). The apparatus, in general, consisted of a blower, an air-flow symmetry control apparatus, a bleed arrangement to eliminate boundary layer at the inlet, a calibrated venturi meter, and adapter ducts. A dummy duct on the left side with an inlet the same as that for the test duct was used to obtain a symmetrical inlet flow. A resistor control valve was provided at the exit of the dummy duct to regulate the flow. (See fig. 6(a).)

Rakes used for measuring duct-inlet and duct-outlet total and static pressures are shown in figures 4, 5, and 7. The reference pressure for use in correlating the rake data was obtained for duct I by use of a total-pressure tube located upstream from the air intake. The reference pressure for duct II was obtained from a shielded total-pressure tube placed in the dummy-duct inlet. (See fig. 3(b).) Wall static-pressure openings placed symmetrically in the dummy duct and in the test duct a short distance downstream from the inlets were used as a guide in establishing symmetry of flow in the combined inlets. (See figs. 3(a) and 5.) Additional instrumentation consisted of two U-tube manometers connected differentially to each pair of wall static-pressure openings, a calibrated venturi meter, a multiple-tube manometer, and a camera arranged to photograph the manometer.

TESTS AND METHODS

Tests were made first to determine the size of the bleeder necessary to remove the boundary layer ahead of the test duct. The bleed width was increased until the deficiency in total pressure of the air flow near the duct wall was reduced to a negligible quantity throughout the entire flow range. The bleed width so determined was used throughout the pressure-loss tests.

After the bleed setting was determined, the resistor control was adjusted for flow symmetry, which was indicated by null readings on the U-tube manometers. Pressure losses in the test ducts were then measured over a range of air-flow rate extensive enough to include important scale effects. In these tests, pressures were measured first at the duct inlet; the inlet rakes were then removed before pressures were measured at the exit to avoid including the wake losses of the inlet rakes in the results. Results were put on a common basis by the use of the reference pressures.

Duct II was tested also with simulated manufacturing roughness in the inlet. This roughness was obtained by a 4-inch coating of No. 60 (0.012-inch average diameter) carborundum grains attached to the surface with shellac. (See fig. 3(b).) After the carborundum was removed, the worst conceivable construction defect was simulated by a brass-rod spoiler of $\frac{3}{16}$ -inch-square section placed in the inlet. (See fig. 3(c).)

RESULTS AND DISCUSSION

Because of the characteristics of the setup, the entry conditions correspond to those for an installation operating with the airplane in level flight at an inlet-velocity ratio near 1. Although the inflow for these tests does not simulate any flight conditions for this airplane, the pressure-loss results are believed to be conservative for the high-speed condition at which the divergence of the entering streamlines would tend to aid the internal diffusion. No serious decrease in duct performance is expected over the very limited range of angle of attack for which high performance is required for such an airplane.

Total Pressure and Velocity Distribution of Duct Exits

A representative distribution of velocity and total-pressure deficiency in the duct exit is shown in figure 8(a) for duct I and in figure 8(b) for duct II. The velocity distribution is presented in terms of the ratio of local velocity to maximum velocity measured at the duct exit $\frac{v_{el}}{v_{e_{max}}}$. The total-pressure deficiency is presented in the form of a local pressure-loss coefficient based on the duct-inlet total and dynamic pressures $\frac{\bar{H}_1 - H_{e1}}{q_1}$. The reductions in local velocity and increases in local pressure-loss coefficients that occur near the wall of the duct appear to be somewhat less for duct II than for duct I.

Pressure Losses

The pressure-loss results are presented in the form of duct pressure-loss coefficients $\frac{\bar{H}_1 - \bar{H}_e}{q_1}$ and absolute pressure losses corrected to standard conditions $\sigma_1(\bar{H}_1 - \bar{H}_0)$. The pressure-loss coefficient has the advantage of becoming approximately independent of air flow at the high rates of flow. The corrected duct pressure loss is necessary to permit direct comparisons of losses for ducts that differ in inlet area.

Duct pressure-loss coefficients based on average pressures are given in figure 9 over a range of air-flow rate for duct I, for duct II, and for duct II with splitter vane, with carborundum grains, and with spoiler. Pressure-loss coefficients for duct I ranged from about 0.52 at an air-flow rate of 4 pounds per second to about 0.19 at an air-flow rate of 27 pounds per second. Above an air-flow rate of 10 pounds per second, the curve tends to flatten out. Because of the slow decrease in pressure-loss coefficient at the high rates of flow, it is believed that this curve may be extrapolated with little error.

The pressure-loss coefficients for duct II (fig. 9) range from 0.17 at an air-flow rate of 4 pounds per second to 0.06 at an air-flow rate of 27 pounds per second. In general, the variation of pressure-loss coefficient with air-flow rate is similar in character for duct II and duct I. Because the inlet areas of the two ducts are not the same, the ratio of pressure-loss coefficients will differ from the ratio of absolute pressure losses at any given air-flow rate.

An increase in pressure-loss coefficient was obtained when the splitter vane was inserted in duct II. At 27 pounds of air flow per second, the pressure-loss coefficient increased from 0.06 without the splitter vane to 0.09 with the vane - a 50-percent increase. (See fig. 9.) This large increase in loss can be attributed to the increase in wetted area and slight decrease in cross-sectional area that resulted from insertion of the vane.

The curve of pressure-loss coefficient obtained for duct II with carborundum grains in the inlet closely approximates that which was obtained for duct II with the splitter vane. (See fig. 9.) Installation of a spoiler around the perimeter of the inlet of duct II produced large increases in the pressure-loss coefficient at all but the very lowest air-flow rate and changed the character of the variation of loss coefficient with air flow. At the highest air flows the pressure-loss coefficient of duct II increased about 700 percent with the addition of the spoiler. The rise in pressure-loss coefficient with increasing air flow, in contrast to the decreasing characteristic obtained without the spoiler, may be indicative of the occurrence of separation and the formation of a flow pattern similar to a vena contracta. On the basis of these results it is desirable to avoid roughness or discontinuities (such as a faulty joint) at the duct inlet.

An arithmetic mean of the pressures was used in computing the pressure-loss coefficients of figure 9 in order to facilitate computation of the urgently needed comparative data. The pressure-loss coefficients for duct II and duct II with splitter vane, the more important ducts, were also computed by flow-weighted integration methods. (See fig. 10.) The pressure-loss coefficients obtained by the integration method for duct II and duct II with splitter vane are about 10 percent greater than those obtained by the arithmetic average.

The variations of corrected duct pressure loss $\sigma_1 (\bar{H}_1 - \bar{H}_0)$ with weight rate of air flow are shown in figure 11, which was derived from the data presented in figure 9. Since the ordinate of figure 11 represents absolute losses instead of coefficients involving the geometry of the inlet, the relative merits of the test configurations can be determined directly from this figure. Duct II is shown to have the lowest losses throughout the entire range of air-flow rate. At 27 pounds of air flow per second, the maximum flow rate tested, the loss in duct I for standard sea-level density at the duct inlet was about 21.5 pounds per square foot, compared with a value of about 8 pounds per square foot for duct II.

CONCLUSIONS

An investigation to determine the pressure losses of intake ducts for a high-speed subsonic jet-propelled airplane indicated the following results expressed in the form of arithmetic pressure averages:

1. The pressure losses for ducts I and II at an air-flow rate of 27 pounds per second were 19 percent and 6 percent, respectively, of the dynamic pressure at the inlet.
2. For standard sea-level inlet conditions, the pressure loss for duct II at the maximum test air-flow rate of 27 pounds per second was about 8 pounds per square foot or only 37 percent of the loss for duct I. This percentage is not the same as the ratio of the losses expressed in percent of the inlet dynamic pressure because of inequality of the duct-inlet areas.
3. The pressure loss for duct II with the splitter vane at an air-flow rate of 27 pounds per second was 9 percent of the dynamic pressure at the inlet, a value 50 percent greater than the loss for duct I.
4. It is highly desirable to avoid roughness or discontinuities (such as a faulty joint) at the duct inlet. A moderate amount of roughness at the inlet increased the duct pressure loss by 50 percent; a sufficiently large inlet discontinuity increased the duct pressure loss by about 700 percent.

Langley Memorial Aeronautical Laboratory
National Advisory Committee for Aeronautics
Langley Field, Va.

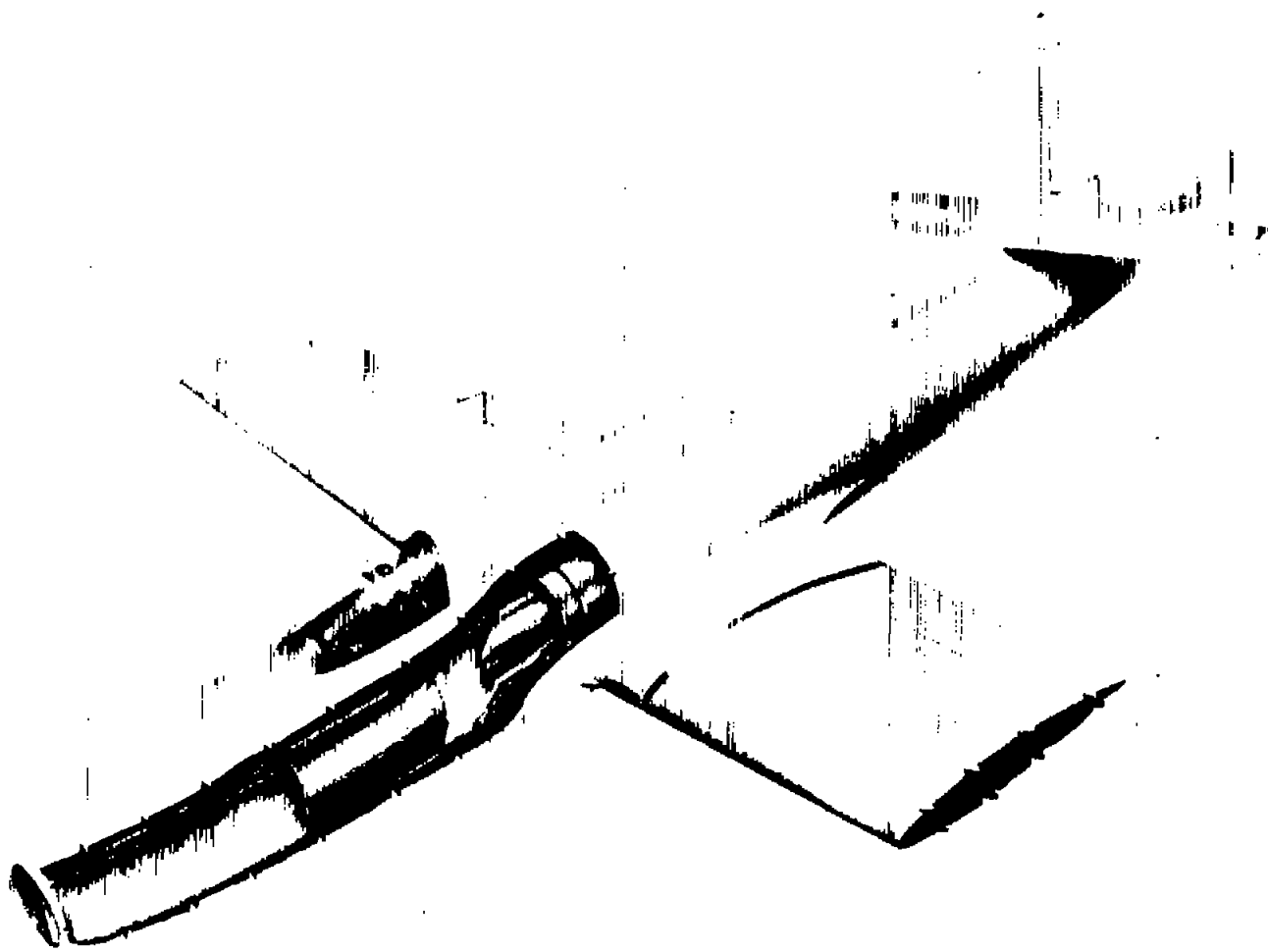
REFERENCES

1. Becker, John V., and Baals, Donald D.: Wind-Tunnel Tests of a Submerged-Engine Fuselage Design. NACA ACR, Oct. 1940.
2. Henry, John R.: Design of Power-Plant Installations. Pressure-Loss Characteristics of Duct Components. NACA ARR No. L4F26, 1944.

TABLE I.- CROSS-SECTIONAL AREAS AND
HYDRAULIC DIAMETERS OF DUCTS

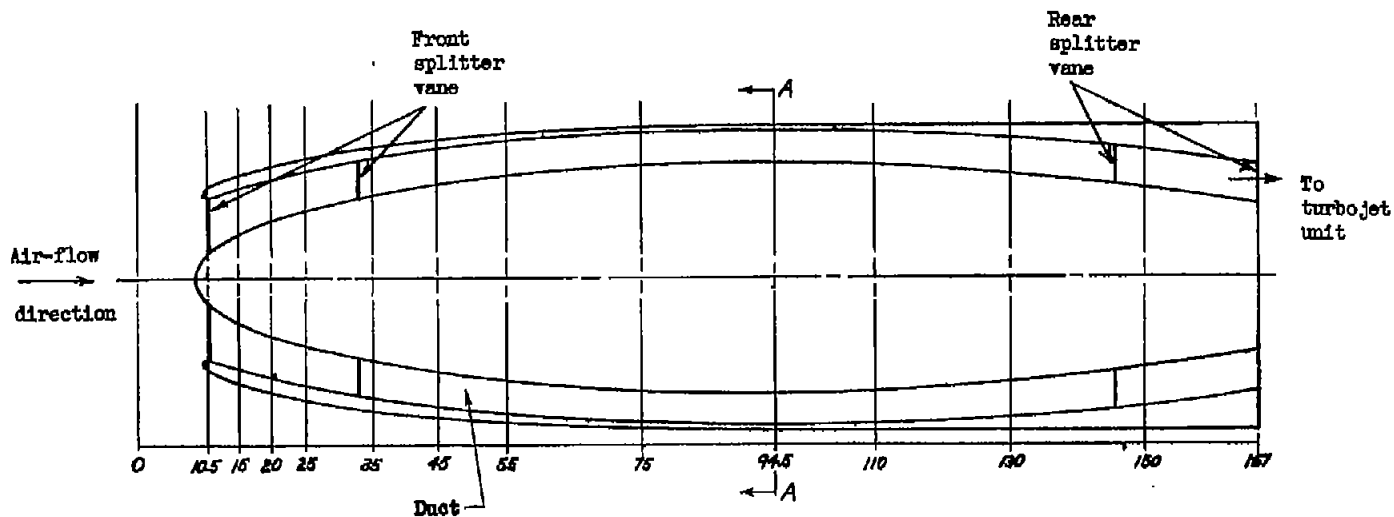
Station	Cross-sectional area (sq in.)	Hydraulic diameter (in.) (a)
Duct I		
10.5	168	9.06
15.0	151	8.28
55.0	151	8.16
94.5	150	7.72
167.0	214	8.40
Duct II		
10.438	151	11.97
15.0	164	12.55
60.0	259	16.42
91.0	284	15.03
160.0	231	12.53
167.0	220	11.05
Duct II with splitter vane		
10.438	151	11.97
15.0	156	9.64
60.0	250	10.90
91.0	278	11.10
160.0	224	10.40
167.0	220	11.05

^aThe hydraulic diameter is 4 times the cross-sectional area divided by the wetted perimeter.

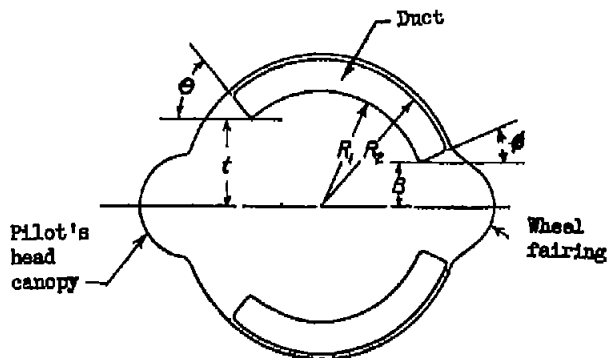


NATIONAL ADVISORY
COMMITTEE FOR AERONAUTICS

Figure 1.- High-speed subsonic jet-propelled airplane with a proposed duct for the air-induction system.



Plan view of duct in fuselage



Section A-A

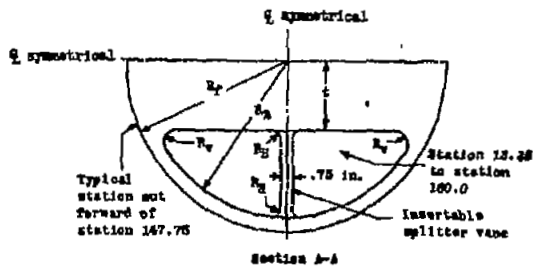
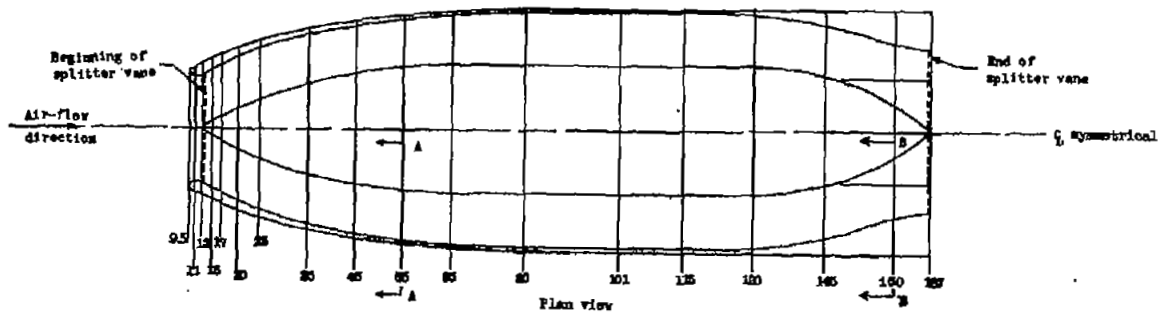
Section of fuselage with duct

Station (in.)	R_1 (in.)	R_2 (in.)	t (in.)	θ (deg)	B (in.)	ϕ (deg)
10.5	3.44	11.25	0.50	2.25	0.30	2.25
15.0	6.10	12.41	1.56	11.00	1.56	11.00
20.0	7.99	13.81	2.69	20.00	2.56	19.50
25.0	9.42	14.88	3.75	23.25	3.44	21.50
35.0	11.55	16.50	5.75	30.00	4.88	25.00
45.0	13.08	17.78	7.50	35.50	5.69	25.00
55.0	14.21	18.75	9.00	39.75	5.94	25.00
75.0	15.58	19.97	11.31	46.50	6.00	25.50
94.5	16.00	20.34	12.00	48.00	6.00	25.50
110.0	15.74	20.31	11.98	45.75	6.00	25.50
130.0	14.57	19.50	8.03	39.50	6.00	24.00
150.0	12.31	17.66	3.19	18.00	3.81	14.00
167.0	10.13	15.50	0	0	0	0

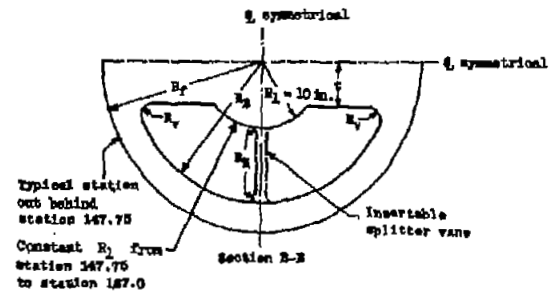
(a) Duct I.

NATIONAL ADVISORY
COMMITTEE FOR AERONAUTICS

Figure 2.- Internal lines of airplane induction system.



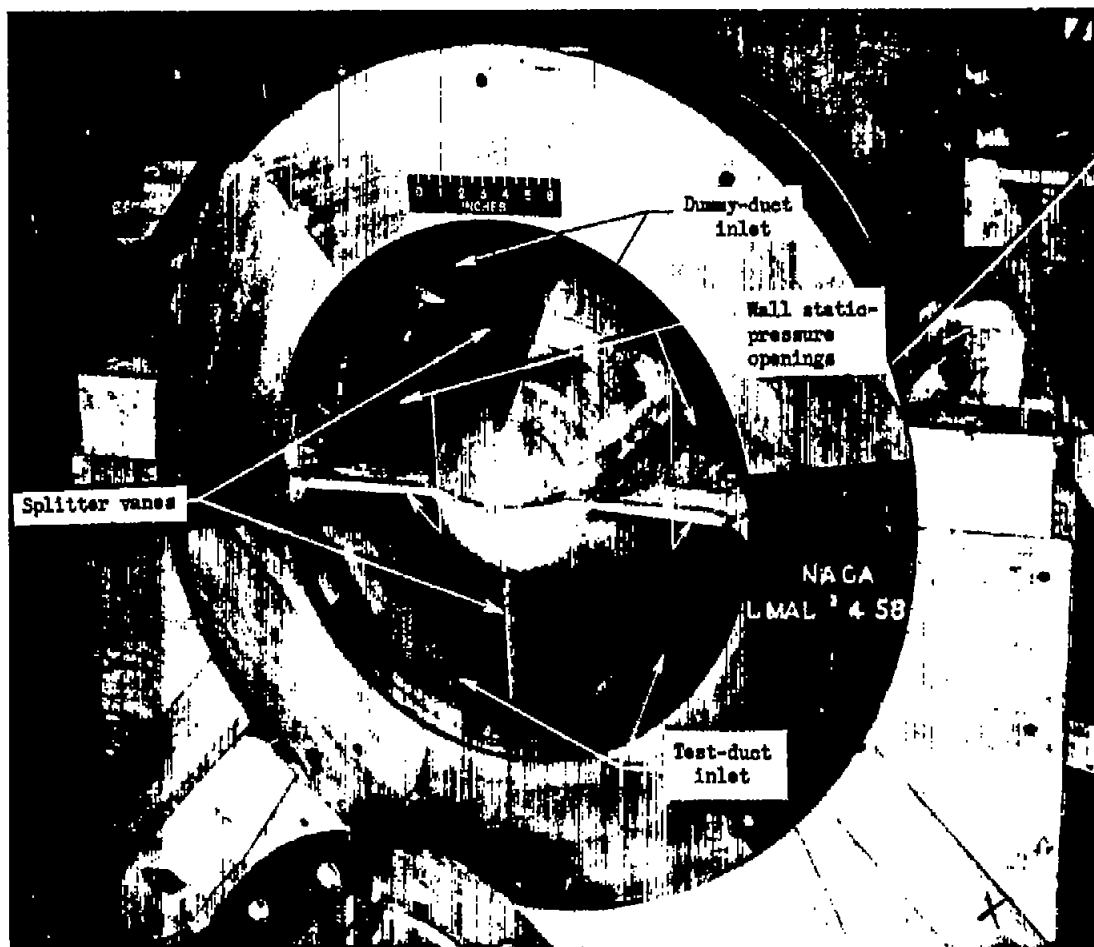
Station (in.)	R_1 (in.)	R_2 (in.)	s (in.)	R_3 (in.)	R_4 (in.)
9.50	10.25	10.25	0	0	0
9.75	11.08	9.94	0	0	0
10.00	11.32	9.85	0	0	0
11.00	12.09	9.83	0	0	0
20.00	15.23	12.23	4.20	.17	.26
30.00	15.89	17.31	7.07	.29	.68
40.00	20.20	19.05	9.83	.57	.85
60.00	21.71	20.95	11.12	.73	1.00
70.00	22.44	22.00	12.42	.92	1.29
91.00	24.00	23.25	12.75	1.00	1.50
104.00	24.00	22.71	12.14	1.00	1.50
140.00	24.00	21.72	11.72	1.00	1.50
160.00	24.00	19.80	9.25	1.00	1.50
160.00	24.00	17.07	4.76	1.00	1.50
187.00	24.00	15.50	0	0	0



(b) Duct II with insertable splitter vane. (Sections are not to scale.)

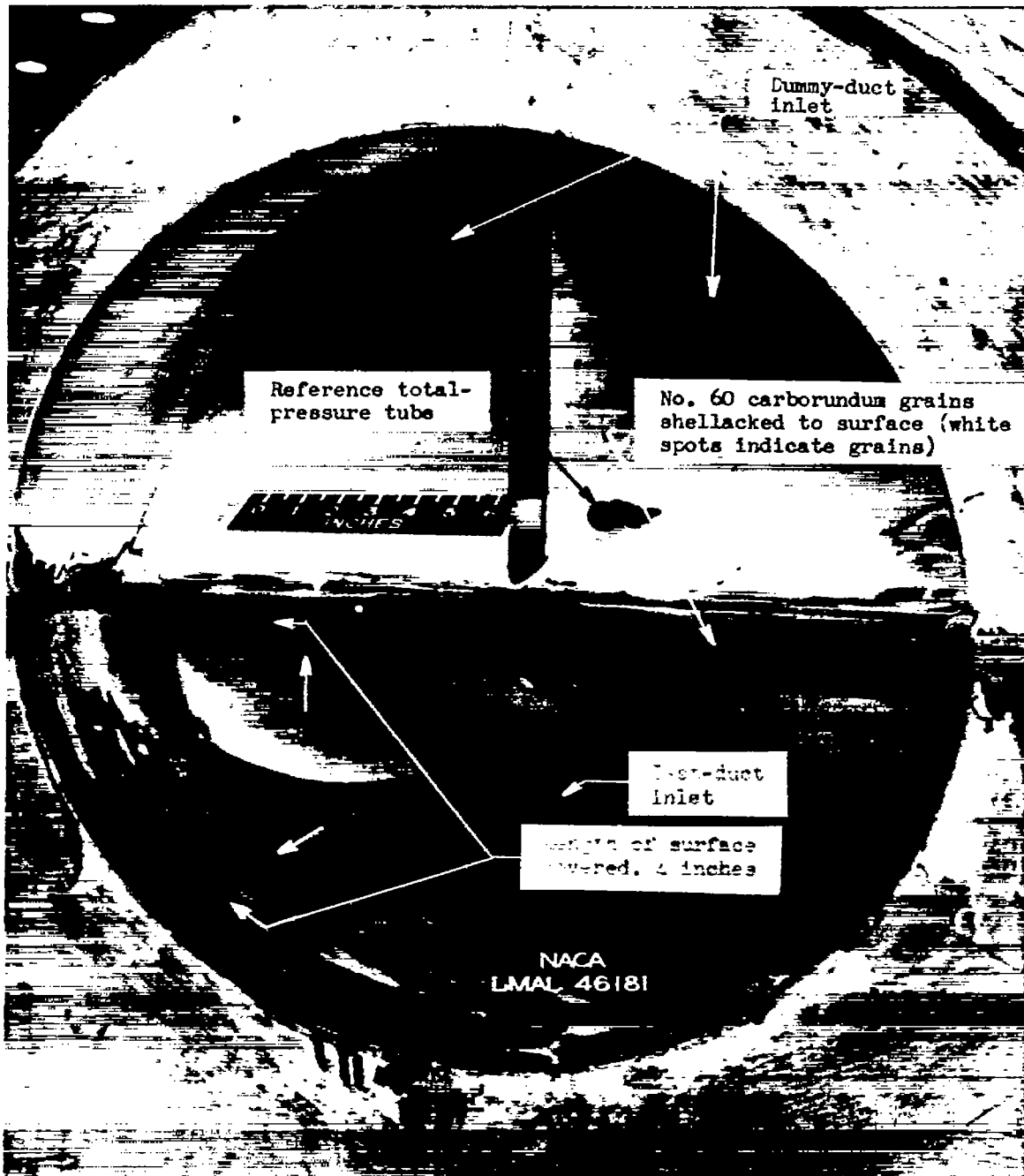
Figure 2.- Concluded.

NATIONAL ADVISORY
COMMITTEE FOR AERONAUTICS

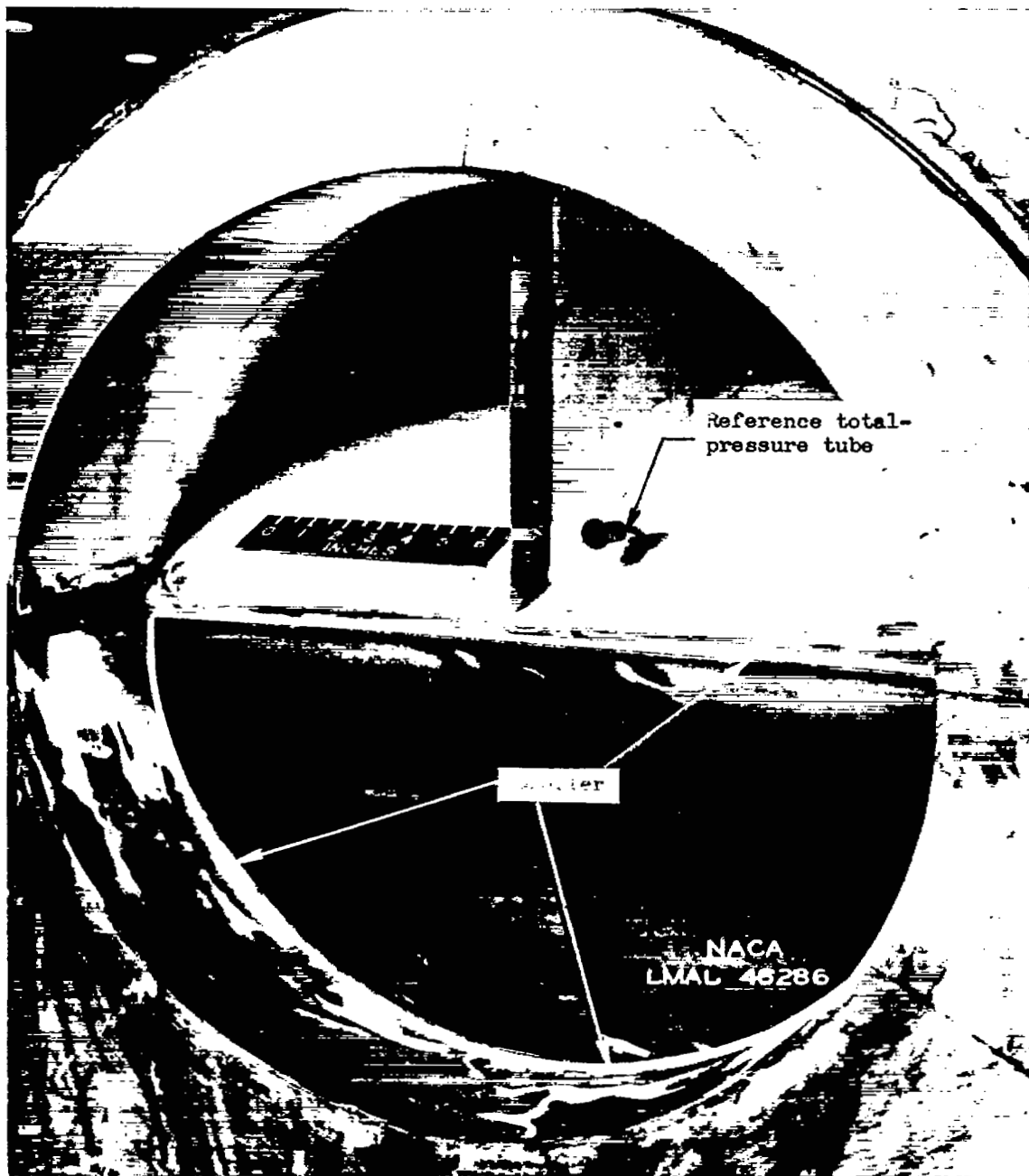


(a) Inlet of duct I.

Figure 3.- Duct inlets.



(b) Inlet of duct II showing carborundum grains on surface.



(c) Inlet of duct II with spoiler.

Figure 3.- Concluded.

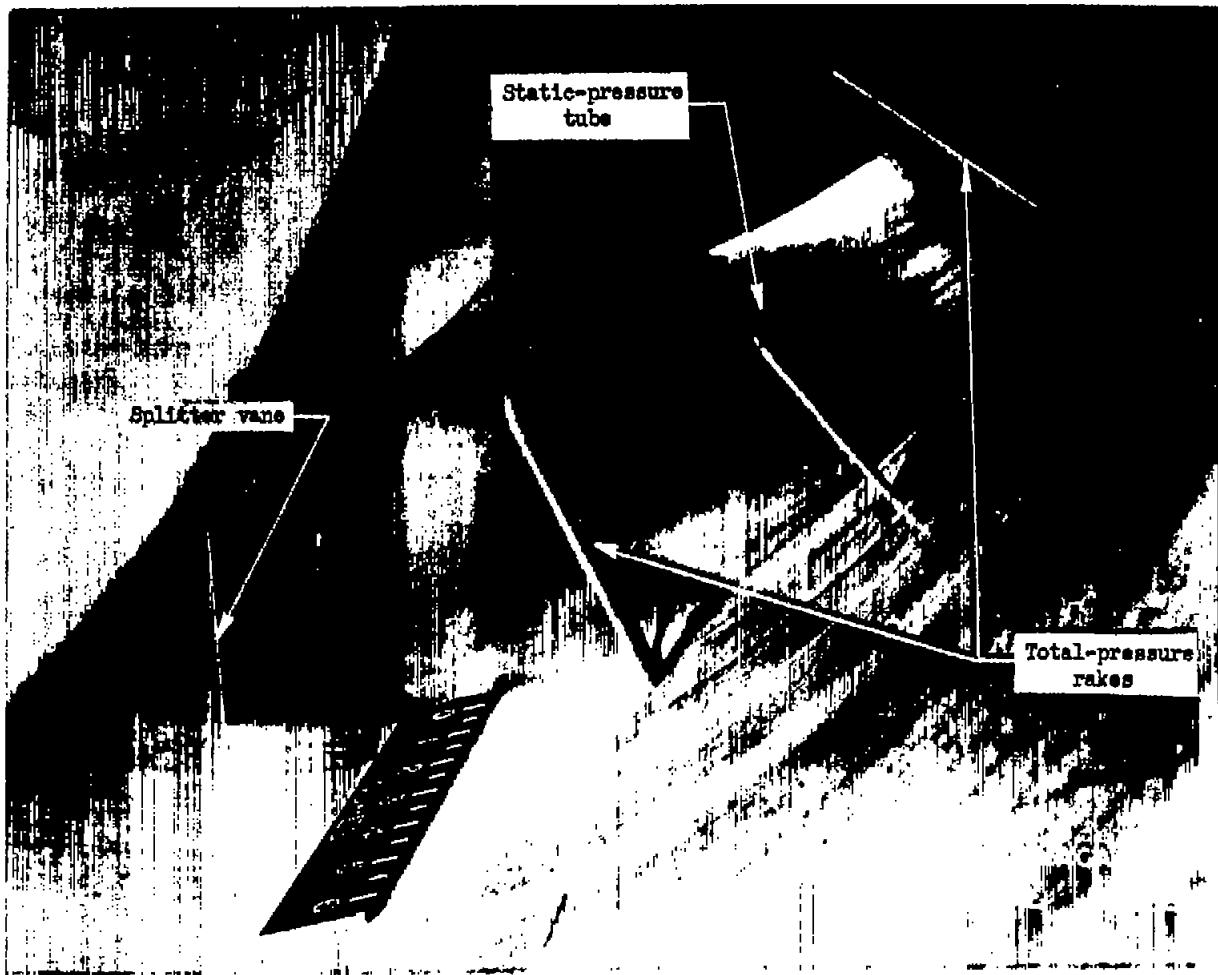


Figure 4.- Exit of duct I showing rakes and splitter vane.

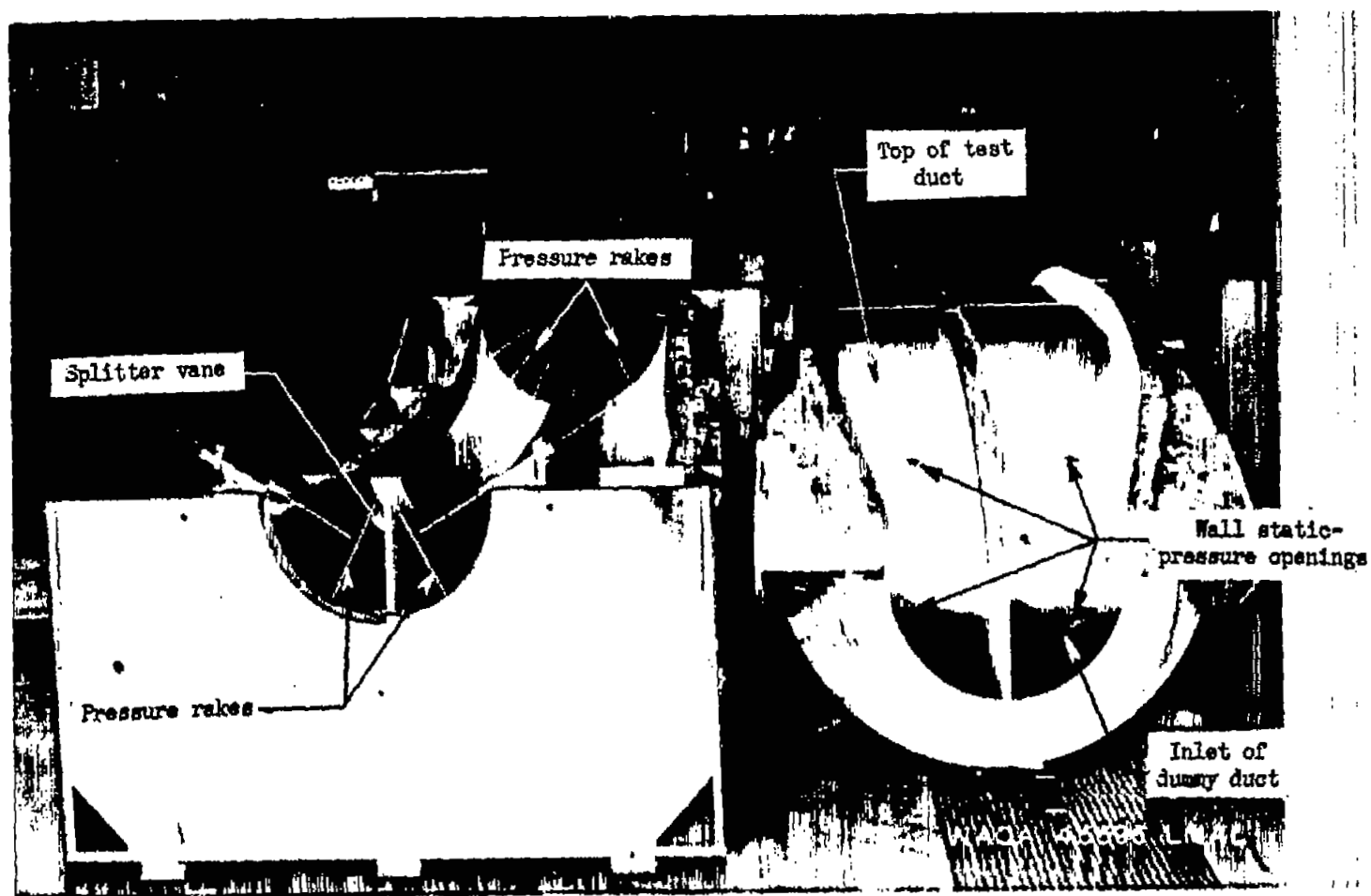
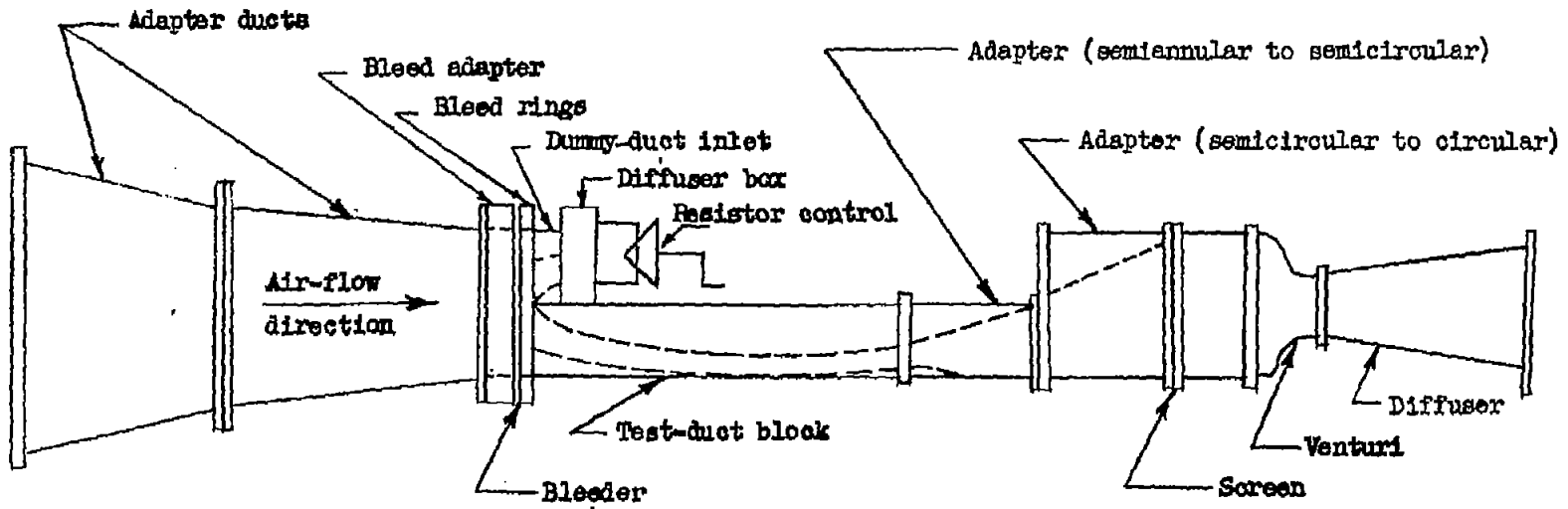


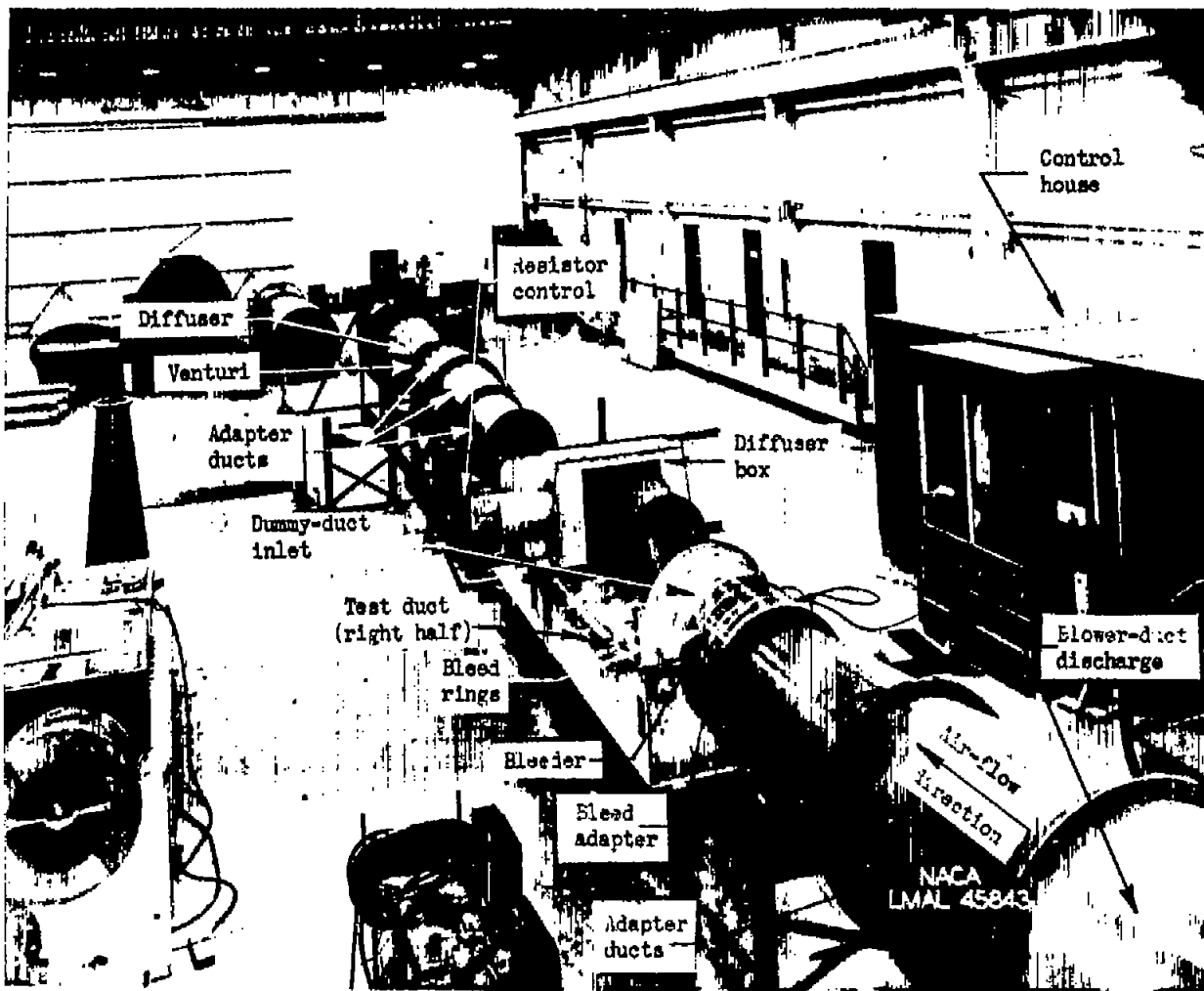
Figure 5.- Disassembled view of duct II with splitter vane installed. Duct lying on its side.



(a) Diagrammatic view.

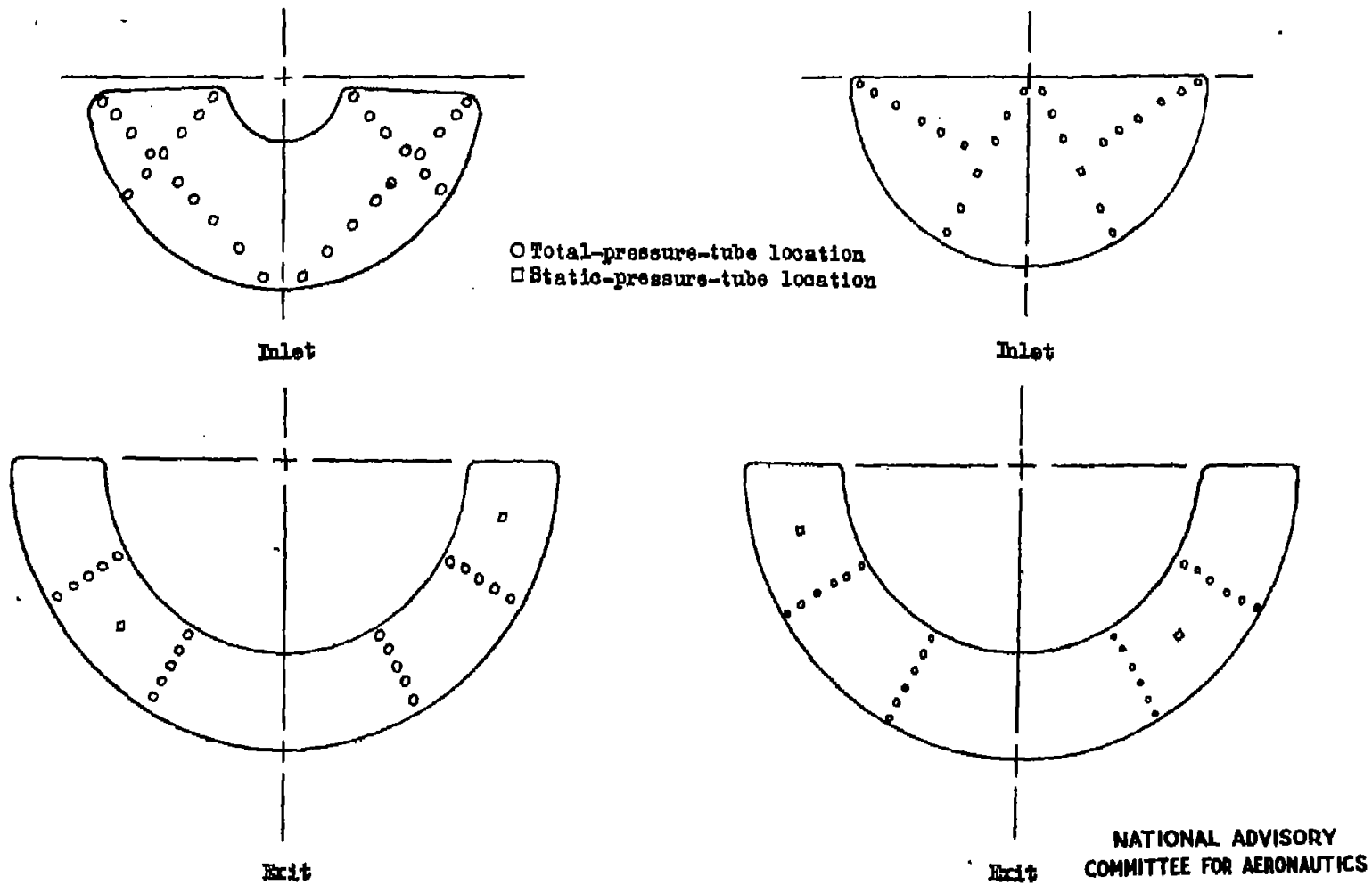
Figure 6.- Test setup.

NATIONAL ADVISORY
COMMITTEE FOR AERONAUTICS



(b) General view.

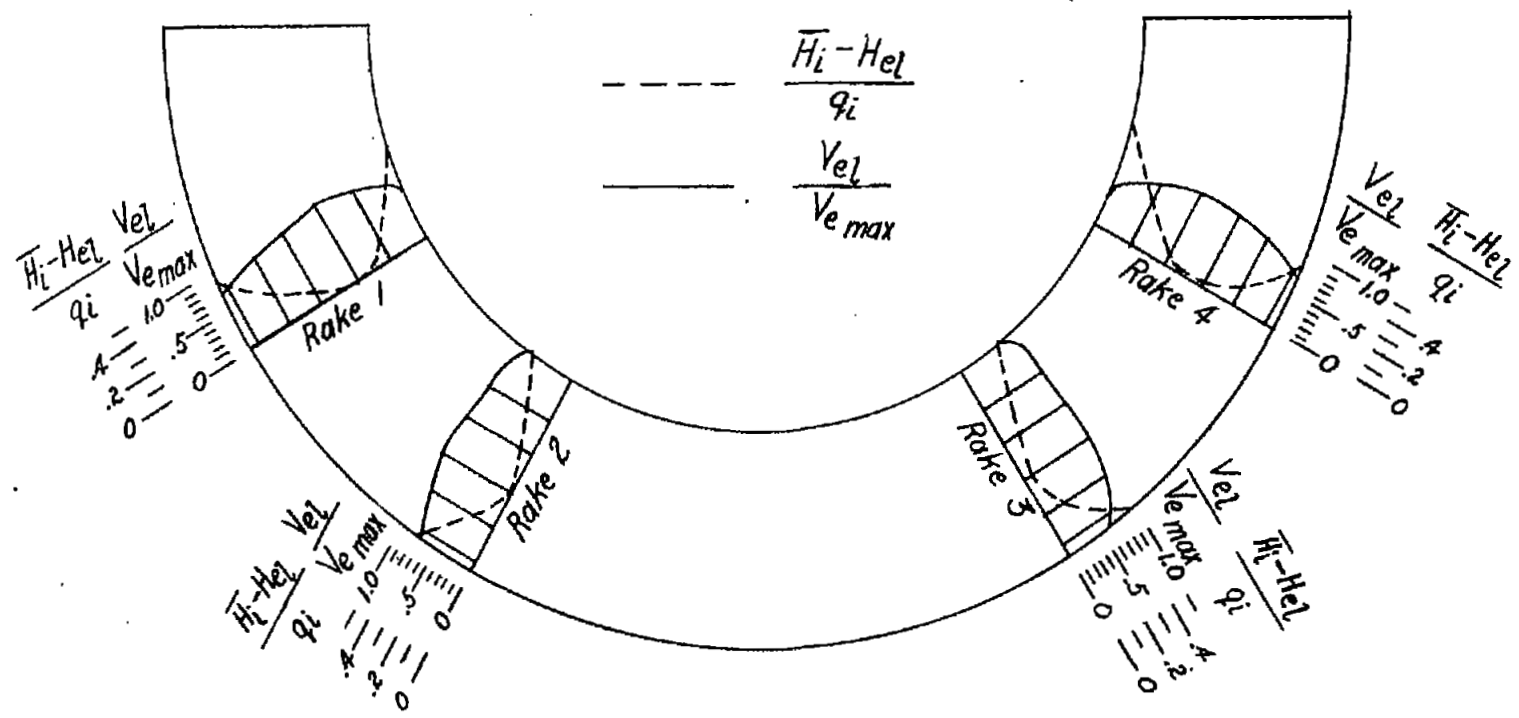
Figure 6.- Concluded.



(a) Duct I:

(b) Duct II.

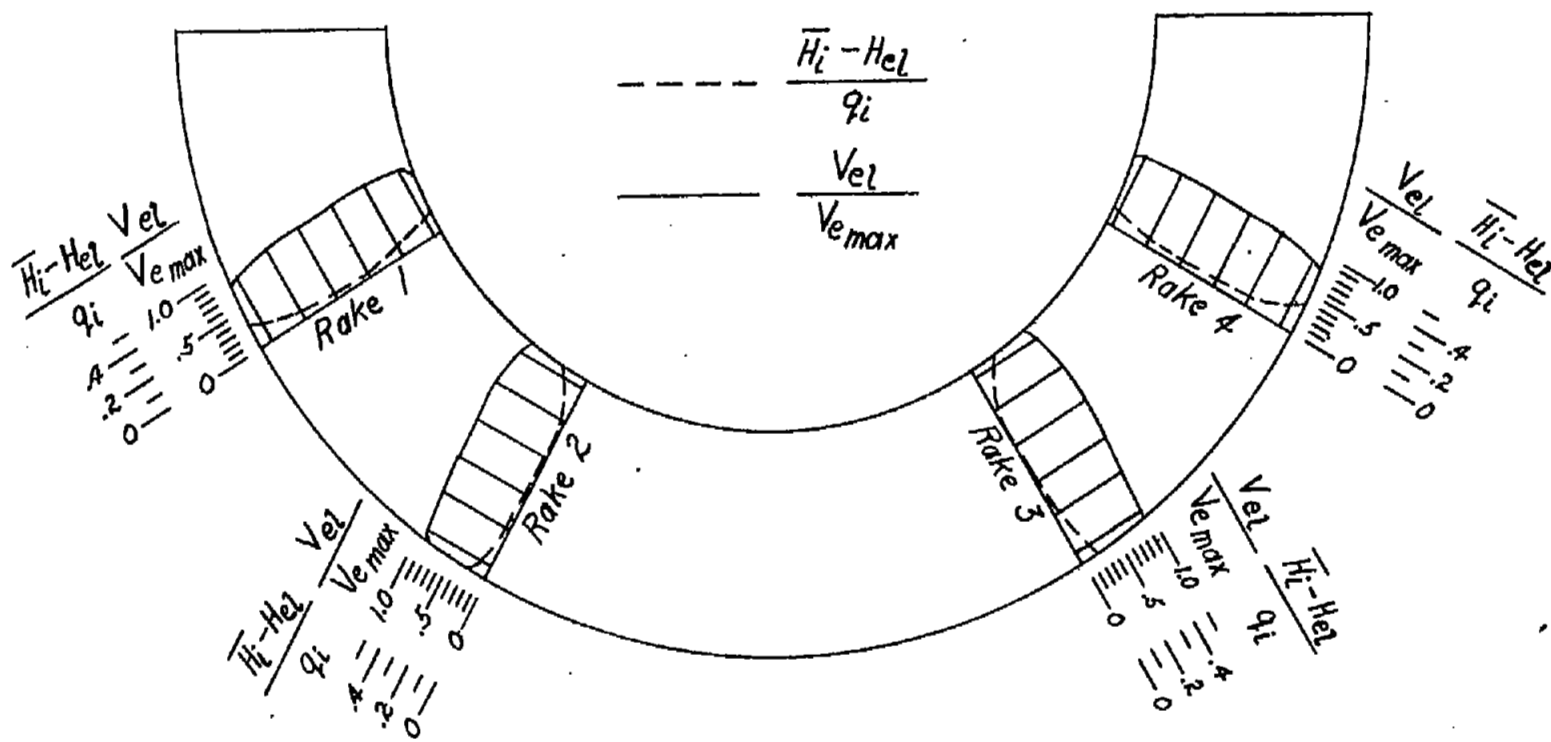
Figure 7.- Locations of total-pressure and static-pressure tubes in inlets and exits of ducts. (Observer looking downstream.)



NATIONAL ADVISORY
COMMITTEE FOR AERONAUTICS

(a) Duct I. $W = 249$ pounds per second; $q_1 = 96.3$ pounds per square foot;
 $V_{max} = 267$ feet per second; $H_1 = 2355$ pounds per square foot.

Figure 8.- Representative velocity and total-pressure profiles of the exits of the ducts.



NATIONAL ADVISORY
COMMITTEE FOR AERONAUTICS

(b) Duct II. $W = 25.7$ pounds per second; $q_1 = 122.4$ pounds per square foot;
 $V_{e max} = 243$ feet per second; $H_1 = 2336$ pounds per square foot.

Figure 8.- Concluded.

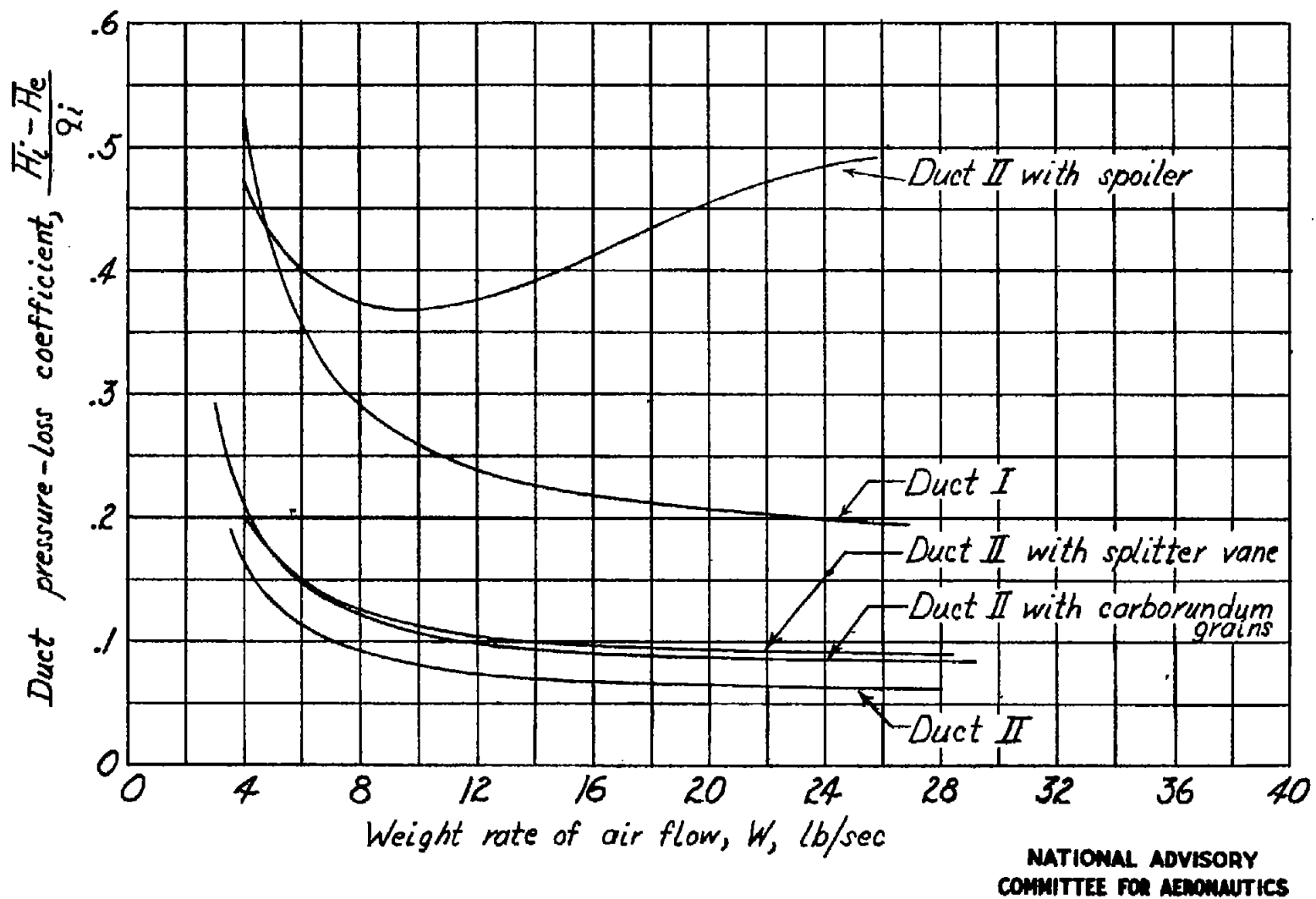


Figure 9.- Variation of duct pressure-loss coefficient with weight rate of air flow.

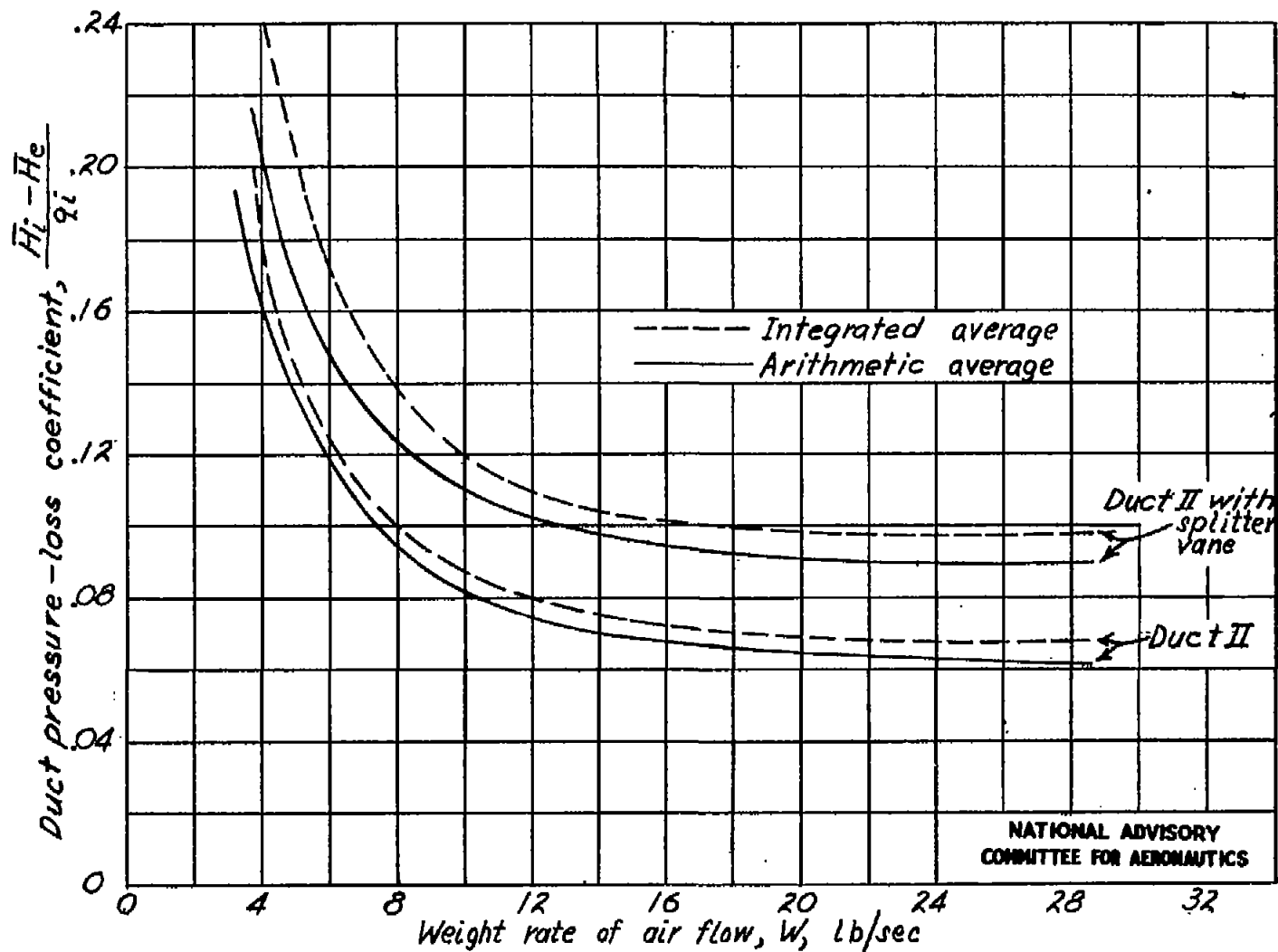


Figure 10.- Comparison of duct pressure-loss coefficients based on integrated and arithmetic averages.

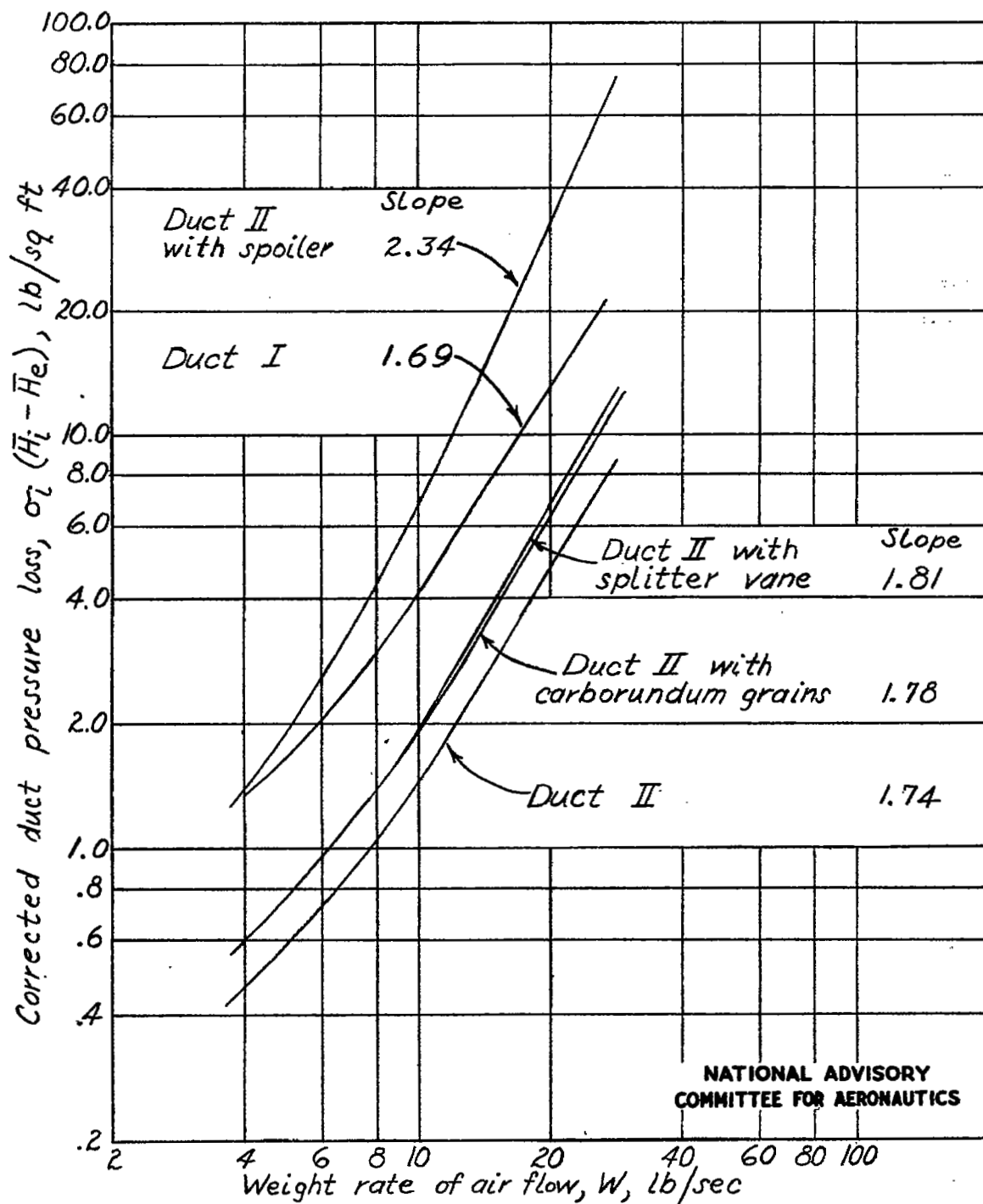


Figure 11.- Variation of corrected duct pressure loss with weight rate of air flow. Slopes measured above 12 pounds per second.

NASA Technical Library



3 1176 01436 3379